Fermi National Accelerator Laboratory

FERMILAB-Conf-97/176-E
CDF and DØ

Electroweak Results from the Tevatron

Mark Lancaster
For the CDF and DØ Collaborations

Lawrence Berkeley Laboratory
Berkeley, California

Fermi National Accelerator Laboratory
P.O. Box 500, Batavia, Illinois 60510

June 1997

Published Proceedings of the *Les Recontres de Physique de la Vallee d'Aoste*,
La Thuile, Italy, March 3-7, 1997

Operated by Universities Research Association Inc. under Contract No. DE-AC02-76CH03000 with the United States Department of Energy

Electroweak Results from the Tevatron [1]

Mark Lancaster

On behalf of the CDF & DØ Collaborations

Lawrence Berkeley Laboratory, Berkeley, California, USA

Abstract

Using data collected from $p\bar{p}$ collisions at the Fermilab Tevatron collider the latest electroweak results from the CDF and DØ collaborations are presented. Measurements of the W and Z boson production cross sections are detailed, which in addition to testing the Standard Model in their own right also allow a determination of the W boson width. Analyses of Drell-Yan production above the Z pole allow limits to be placed on the existence of neutral gauge bosons beyond the Standard Model and parton compositeness. A first measurement of the forward backward asymmetry of the Drell-Yan lepton pairs above the Z pole is also presented. The latest measurements from both collaborations of the W mass are described, which when averaged yield a W mass value of 80.375 ± 0.100 GeV/c^2.

[1] Presented at Les Recontres de Physique de la Vallée d'Aoste, La Thuile, Italy, March 3-7 1997.

1 Introduction

The electroweak results presented in this paper are based on data taken from $p\bar{p}$ collisions at $\sqrt{s} = 1.8$ TeV at the Fermilab Tevatron collider. The analyses use data taken in two periods, referred to as run-1A (1992-1993) and run-1B (1994-1995). The results from run-1A are published whereas some of the results described from run-1B are still preliminary. The two experiments accumulated data sets with integrated luminosities of 15, 20 pb^{-1} (DØ, CDF) and 80, 90 (DØ, CDF) pb^{-1} in run-1A and run-1B respectively.

2 W and Z cross sections

The W and Z production cross sections are measured through the $W \rightarrow e\nu$, $Z \rightarrow e^+e^-$, $W \rightarrow \mu\nu$ and $Z \rightarrow \mu^+\mu^-$ decay modes. Events are selected by demanding a single isolated high P_T charged lepton in conjunction with missing transverse energy (W events) or a second high P_T lepton (Z events). P_T, $\not{E}_T$ cuts for the analyses are 20 (CDF) and 25 GeV/c (DØ). The dominant error in the cross section ($\times$ leptonic branching ratio) determination arises from the uncertainty in the integrated luminosity which is 3.6 % for CDF and 5.4 % for DØ. In figure 1 the published 1A [1, 2] and the preliminary DØ run-1B measurements are compared to the $\mathcal{O}(\alpha_s^2)$ prediction [3]. The shaded region in the figure represents the theoretical uncertainty which arises principally from the uncertainty in the parton distribution functions.

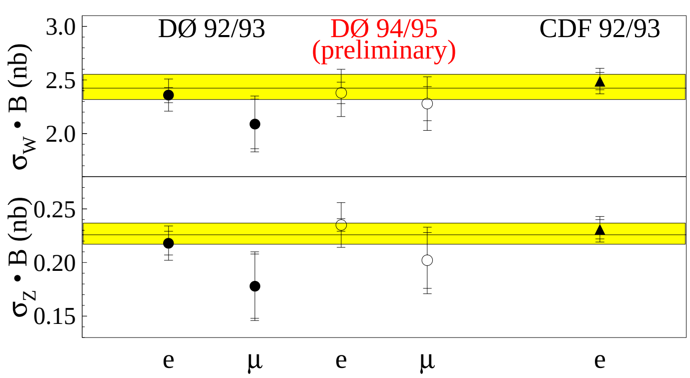

Figure 1: The W and Z cross sections in the leptonic decay mode measured by CDF and DØ compared to the $\mathcal{O}(\alpha_s^2)$ theoretical prediction (shaded region).

3 W width measurement

The measured W and Z production cross sections can be used to make an indirect determination of the W width through the relation :

$$\Gamma_W = \frac{\sigma_W}{\sigma_Z} \cdot \frac{\Gamma(W \to l\nu)}{B(Z \to ll)} \cdot \frac{1}{R}$$

where R is ratio of the W and Z cross sections for W and Zs decaying leptonically i.e. R = $\frac{\sigma_W \cdot B(W \to l\nu)}{\sigma_Z \cdot B(Z \to ll)}$. The method has the advantage that many sources of experimental systematic error cancel in R, in particular the luminosity uncertainty. However the method does rely on quantities calculated within the Standard Model (SM) namely $\sigma_W/\sigma_Z = 3.33 \pm 0.03$ [3] and $\Gamma(W \to l\nu) = 225.2 \pm 1.5$ MeV [4] as well as the LEP measurement of B(Z $\to ll$) [5]. The measurements are summarised in figure 2. The world average is $\Gamma_W = 2.062 \pm 0.059$

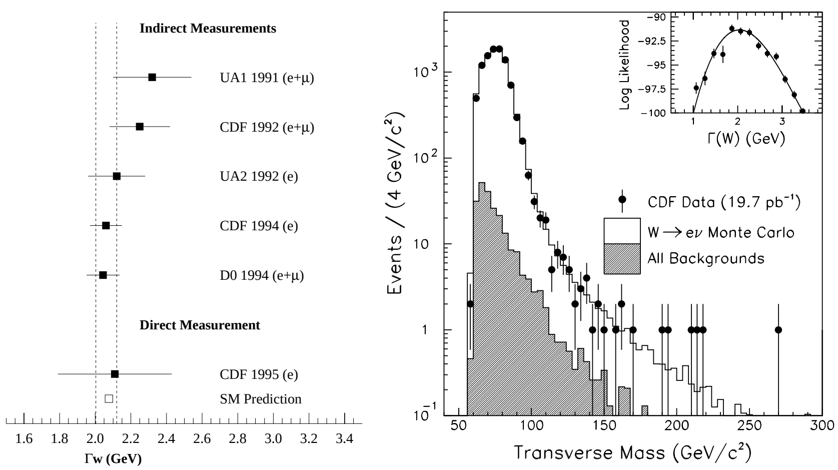

Figure 2: Left : A summary of the W width determinations. The dotted lines delimit the world average value. Right : The transverse mass distribution used by CDF to determine the W width.

GeV [2] which when compared to the SM prediction of 2.077 ± 0.014 GeV [4] excludes at the 95% confidence level non SM decays contributing > 109 MeV to the observed width. A less model dependent determination of the W width has been performed by CDF from a measurement based on the W transverse mass (M_T) line shape. The transverse mass is defined as the invariant mass in the transverse plane of the lepton and the neutrino from the W decay. At high values of M_T the Breit Wigner dominates over the detector resolution and determines the M_T shape. From a fit in the region $M_T > 110$ GeV/c^2 the width is determined to be , $_W = 2.11 \pm 0.28 \pm 0.16$ GeV [6]. Although not statistically competitive with the width measurement using R, the measurement has the advantage that it is relatively free from SM assumptions.

4 Drell-Yan Production

The large center of mass energy available in parton-parton collisions at the Tevatron allows searches of parton substructure to be made to an unprecedented level. The Drell-Yan process ($q\bar{q} \rightarrow \gamma/Z \rightarrow l^+l^-$) provides a particularly clean environment to make such searches. In the region above the Z pole, where the $\gamma - Z$ interference effects are strongest, the presence of parton substructure would modify the predicted Drell-Yan cross section. The modification to the cross section is dependent upon both the scale at which the substructure would be revealed (Λ) and the phase of the interference. Using both run-1A and run-1B data CDF has made measurements of the differential Drell-Yan cross section, $d^2\sigma/dMdy$, in the mass range $10 < M_{ll} < 550$ GeV/c^2 [7]. The results are compared in figure 3 with both the SM prediction and the predictions of a particular compositeness model [8]. From the combination of electron and muon data

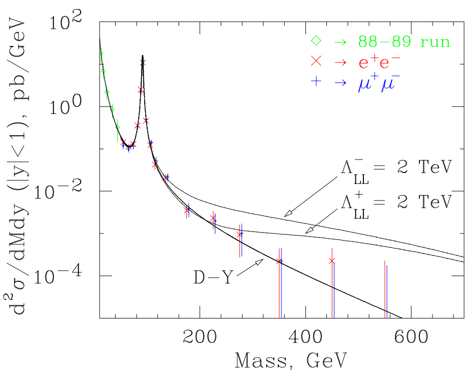

Figure 3: The double differential Drell-Yan cross section for CDF electron and muon data. The SM prediction (denoted by D-Y) is shown along with the prediction of a particular compositeness model.

CDF obtains compositeness limits, for left handed contact interactions, of : $\Lambda_+ > 3.1$ TeV and $\Lambda_- > 4.3$ TeV, for constructive and destructive interference respectively; indicating the absence of substructure down to a spatial scale of 10^{-17}cm. By considering deviations from the SM cross section predictions, it is also possible to place a limit on the existence of additional neutral gauge bosons. Both experiments have performed such an analysis and exclude additional neutral gauge bosons with masses $>$ 690 GeV/c^2 (CDF [9]), 670 GeV/c^2 (DØ [10]) at the 95% confidence limit.

5 Forward-Backward Asymmetry

In addition to a direct search for physics beyond the Standard Model from a measurement of the Drell-Yan differential cross section, an examination of the forward-backward asymmetry of the lepton pairs in the parton center of mass frame also has the potential to reveal new physics. The measurement complements the analogous measurements made at LEP and SLC. In the e^+e^- measurement fragmentation uncertainties dominate the error whereas at the Tevatron the uncertainty arises from the parton distribution functions since the Drell-Yan production integrates over $u\bar{u}$ and $d\bar{d}$ interactions. The forward-backward asymmetry, A_{FB}, is defined as :

$$A_{FB} = \frac{\sigma_F - \sigma_B}{\sigma_F + \sigma_B}$$

where $\sigma_{F(B)}$ is the cross section of leptons produced in the forward (backward) hemisphere in the parton center of mass frame. A_{FB} in the large mass region is a direct probe of the relative strengths of the vector and axial-vector couplings. A_{FB} has a strong energy dependence owing to the change of the Z polarisation as function of center of mass energy. This is illustrated in figure 4 where the SM prediction for A_{FB} is shown as a function of the center of mass energy along with the measurement made by CDF using the entire run-1 data set. The data sample comprises of 183 (e^+e^-) events in the region $M_{ee} > 105$ GeV/c^2 and 5463 in the Z pole region, $75 < M_{ee} < 105$ GeV/c^2. Models with additional neutral gauge bosons can substantially alter A_{FB}. Thus although the asymmetry in the high mass region is currently measured with a rather large error, the measurement has the potential with larger statistics to probe extensions to the SM. This is illustrated in figure 4 where the parton level forward backward asymmetry is shown for three particular extensions to the standard model which have an additional neutral gauge boson.

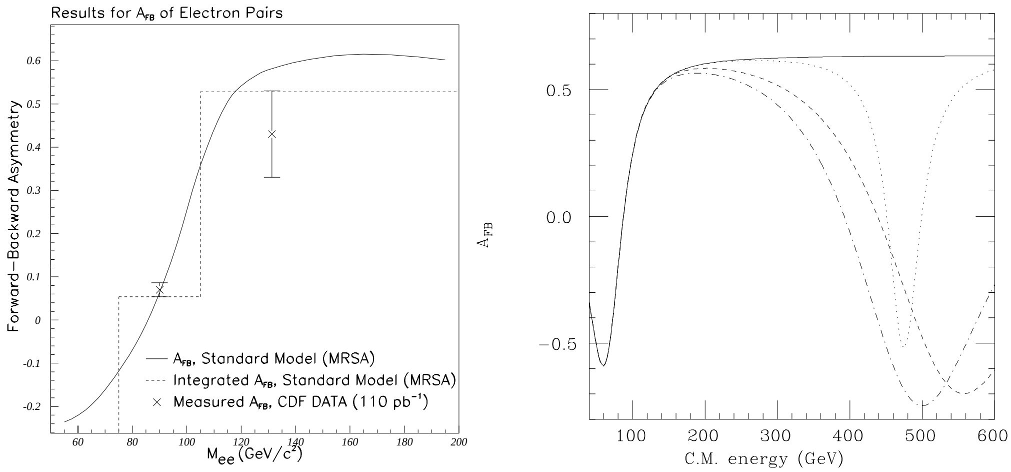

Figure 4: Left : The measured forward backward asymmetry compared to the SM prediction. Right : The predicted asymmetry for three possible extensions to the Standard Model which contain additional neutral gauge bosons of mass 500 GeV/c^2 arising from SO(10) and E(6) extensions to the SM. The solid line is the SM prediction.

6 W mass Measurements

A precise W mass measurement allows a stringent test of the SM beyond tree level where radiative corrections lead to a dependence of the W mass on both the top quark mass and the mass of the, as yet unobserved, Higgs boson. The dependence of the radiative corrections on the Higgs mass is only logarithmic whilst the dependence on the top mass is quadratic. Simultaneous measurements of the W and top masses can thus ultimately serve to constrain the Higgs mass and indicate the existence of particles beyond the Standard Model. To achieve the same sensitivity to the Higgs mass which the current uncertainty on the top mass [13] provides, a W mass measurement with an error of $\mathcal{O}(50)$ MeV is required. As will be shown this limit is rapidly being approached.

Owing to the small backgrounds and superior resolution the W mass is measured from its leptonic decay. Experimentally one cannot determine the longitudinal neutrino momentum and as such one must determine the W mass from transverse quantities namely : the transverse mass (M_T), the charged lepton P_T (P_T^l) or the missing transverse energy ($\not{E}_T$). $\not{E}_T$ is inferred from a measurement of P_T^l and the remaining P_T in the detector, denoted by $\vec{\mathrm{U}}$ i.e.

$$\vec{\not{E}}_{\mathrm{T}} = -(\vec{\mathrm{U}} + \vec{\mathrm{P}}^{l}_{\mathrm{T}}) \qquad \text{and } \mathrm{M_T} \text{ is defined as}$$

$$\mathrm{M_T} = \sqrt{2\mathrm{P}^{l}_{\mathrm{T}}\not{E}_{\mathrm{T}}(1 - \cos\phi)} \qquad \text{where } \phi \text{ is the angle between } \vec{\not{E}}_{\mathrm{T}} \text{ and } \vec{\mathrm{P}}^{l}_{\mathrm{T}}$$

$\vec{\mathrm{U}}$ is composed of the particles comprising the W recoil and the underlying event which experimentally cannot be distinguished. Owing to the contribution from the underlying event the missing transverse energy resolution has a significant luminosity dependence. $\mathrm{M_T}$ is to first order independent of the transverse momentum of the W ($\mathrm{P^W_T}$) whereas $\mathrm{P}^{l}_{\mathrm{T}}$ is linearly dependent on $\mathrm{P^W_T}$. For this reason, and at the current luminosities where the effect of the $\not{E}_{\mathrm{T}}$ resolution is not too severe, the transverse mass is the preferred quantity to determine the W mass.

The W mass itself is determined through a precise simulation of the transverse mass line-shape, which exhibits a Jacobian edge at $\mathrm{M_T} \sim \mathrm{M_W}$. The simulation of the line-shape relies on a detailed understanding of the detector response and resolution to both the charged lepton and the recoil particles.

In the following sections the latest W mass measurements from both collaborations using run-1B data will be presented. The run-1A analyses are already published [14]. The DØ measurement is based on 76 pb^{-1} and uses the $\mathrm{W} \rightarrow e\nu$ channel and has been documented previously [15]. The CDF measurement is based on 90 pb^{-1} and uses the $\mathrm{W} \rightarrow \mu\nu$ channel and is documented here for the first time. The CDF analysis of the $\mathrm{W} \rightarrow e\nu$ channel is still being undertaken.

6.1 Momentum and Energy Scale of Charged lepton

In CDF the momentum scale is set by comparing the J/ψ mass measured from the $\mu\mu$ decay with the world average value. The mass is measured by comparing the measurement with a simulation where the mass is a free parameter. For a reliable mass determination to be made it is essential that the simulation include all the effects in the data which can bias the mass. This includes the effect of B decays, QED radiative corrections and energy loss (dE/dx) in the inactive material prior to the tracking detector. The B decays are a source of bias since CDF uses the beam position in the track fit to improve the momentum resolution. Consequently tracks not originating from the beam position can have a biased momentum measurement when beam constrained. A failure to simulate the effect of B decays can shift the J/ψ mass by ~ 1 MeV ($\equiv 26$ MeV in $\mathrm{M_W}$). A correct simulation of the dE/dx energy loss relies on an accurate knowledge of the type, position and total amount of material the muons traverse prior to the tracking detector. The amount of material is determined from a measurement of the rate of hard bremsstrahlung events by considering the electrons in $W \rightarrow e\nu$ events which have a large E/p value (E/p > 1.2), where E is the energy measured in the calorimeter (which typically includes the bremsstrahlung photon) and p is the momentum measured in the tracking detector. The material location is determined by considering the r-ϕ origin of e^+e^- photon conversion pairs. A failure to account for the dE/dx correction would shift the J/ψ mass by 4 MeV. CDF has $\sim$ 250,000 J/$\psi \rightarrow \mu\mu$ events which allows a rigorous examination of a large number of systematic effects. The largest systematics arise from the simulation of the dE/dx energy losses ($\Delta M_{J/\psi} = 1$ MeV) and the uncertainty in extrapolating the momentum scale ($\Delta M_{J/\psi} = 1$ MeV). The momentum scale is set at the P_T of the J/ψ muons ($P_T \sim 3.5$ GeV/c), whereas the P_T of the muons in W decays is $\sim$ 38 GeV/c. The statistical uncertainty is negligible. The CDF J/ψ sample used to set the momentum scale is shown in figure 5 with the best fit from the simulation. By normalising to the world average J/ψ mass the correction to the measured momentum is determined to be : 1.00023 ± 0.00048 equivalent to a W mass correction of 18 ± 40 MeV. The P_T dependence

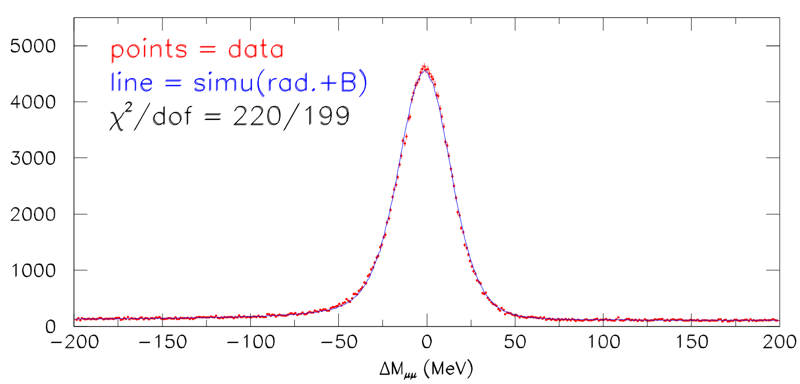

Figure 5: The CDF J/ψ sample used to determine the momentum scale along with the best fit from the simulation. The best fit mass is 3096.2 MeV. $\Delta M_{\mu\mu}$ is the difference between the measured (or simulated) mass and the world average value.

of the momentum scale has been investigated by considering the J/ψ mass as a function of P_T and also by considering the masses of the $\Upsilon(1S)$ and the Z. This is shown in figure 6. The observed dependence with P_T is not corrected for, but is included in the systematic error.

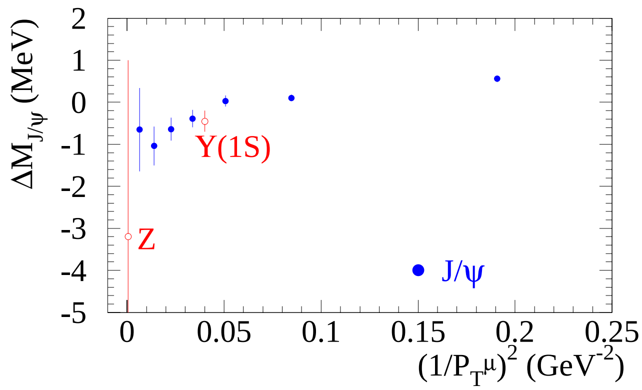

Figure 6: The difference between the observed $\mu\mu$ mass and the world average value expressed as a shift in the J/ψ mass, as a function of $1/{P_T}^2$. The W mass is measured at $1/{P_T}^2 \sim 0.0007$ GeV^{-2}

In DØ the energy scale is principally determined by normalising the measured $Z \rightarrow e^+e^-$ mass to the LEP value. On the basis of test beam studies, the calorimeter response is assumed to have a form :

$$E(\text{meas}) = \alpha \cdot E(\text{true}) + \delta \quad .$$

δ is determined primarily from a mass measurement of the low mass resonances : $\pi^0 \rightarrow \gamma\gamma$ and $J/\psi \rightarrow e^+e^-$. The scale, α, is set from the measured $Z \rightarrow e^+e^-$ mass once δ is determined. In figure 7 the sample of $Z \rightarrow e^+e^-$ used in the calibration is shown along with the range in α and δ implied by the three calibration samples. The uncertainty in the energy scale is 80 MeV and arises principally from the limited Z statistics.

Both experiments determine the charged lepton resolution by a line-shape fit to the Z events. The error is limited purely by the Z statistics.

6.2 Recoil Model

In order to simulate the $\not{E}_T$ response and resolution it is necessary to have a model for the detector response to the W recoil and underlying event particles. Both experiments use a NLO calculation [16, 17] differential in rapidity as a basis for the generation of P_T^W and use Z and minimum bias data to determine the detector response and resolution to a given P_T^W. At low P_T^W it is necessary to include the effects of multiple soft gluon emissions. This calculation involves the introduction of an ad-hoc non perturbative function [18, 17]

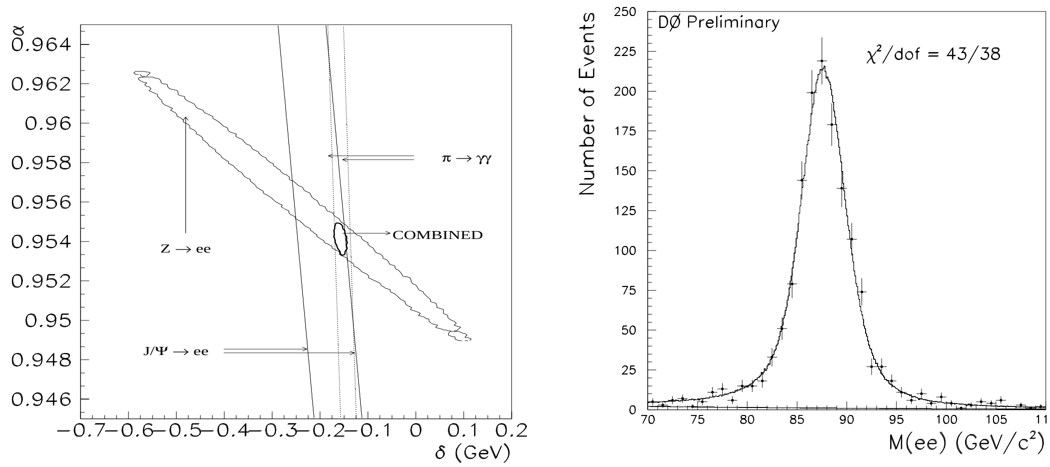

Figure 7: Left : Allowed region of α and δ determined from $J/\psi \rightarrow e^+e^-$, $\pi^0 \rightarrow \gamma\gamma$ and $Z \rightarrow e^+e^-$ decays. Right : The $Z \rightarrow e^+e^-$ events used in the DØ energy calibration.

which can only be determined from data. Both collaborations use the observed P_T^Z spectra to constrain this non perturbative function. Owing to the limited Z statistics there is thus some uncertainty in the from of the true P_T^W spectrum. This uncertainty enters into the final W mass uncertainty. In figure 8 the best fit P_T^Z spectrums are shown for the two collaborations. The calorimeter response to the recoil and underlying event is determined by studying Z events. Since on average the underlying event contribution to $|\vec{U}|$ is zero, a comparison of $<|U|>$ (i.e. P_T^Z calculated from the recoil) to P_T^Z calculated from the leptons is sufficient to determine the response. The comparison is done along the angular bisector of the lepton directions (the so called η axis) to minimise the contribution from the lepton resolution in the determination of P_T^Z. The contribution to $\vec{U}$ from the underlying events is taken from minimum bias data and the contribution to the resolution of the $\not{E}_T$ vector is determined by examining the width of the $\vec{U}$ distribution projected along the η axis. Since the number of underlying events in the data is dependent on the luminosity, the resolution will have a luminosity dependence. In figure 9 the distributions used by CDF and DØ to determine the detector response and resolution to the recoil are shown.

6.3 Parton distributions : W charge asymmetry

The parton distribution functions (pdfs) determine the rapidity distribution of the W and hence of the charged lepton. Both experiments require the charged lepton to be in the

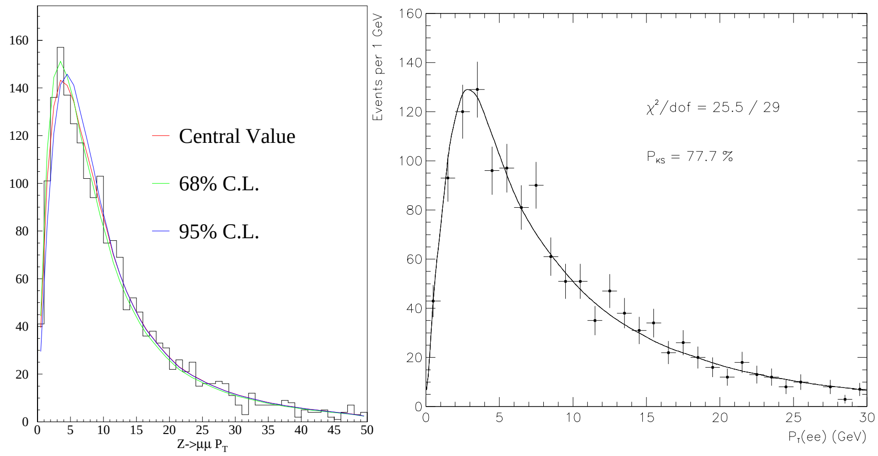

Figure 8: The CDF (left) and DØ (right) P_T^Z data along with the best fit curves obtained by varying the form of the non perturbative function.

central region of the detector ($|\eta| \lesssim 1$) and hence effectively have a rapidity cut on the sample. The simulation of this cut is therefore affected by the choice of pdfs. On average the u quark is found to carry more momentum than the d quark resulting in a charge asymmetry of the produced W i.e. $W^{+(-)}$ are produced preferentially along the p ($\bar{p}$) direction. Since the V-A structure of the W decay is well understood, a measurement of the charged lepton asymmetry therefore serves as a reliable means to constrain the pdfs. The quantity determined experimentally is :

$$A(y_l) = \frac{dN^+(y_l)/dy_l - dN^-(y_l)/dy_l}{dN^+(y_l)/dy_l + dN^-(y_l)/dy_l}$$

where $N^{+(-)}$ is the number of positively (negatively) charged leptons detected at pseudo-rapidity y_l. Since the measurement is a ratio it is relatively free of systematic uncertainties and the dominant error is statistical. The results obtained by CDF [19] using the entire run-1 data are compared to the predictions of the NLO DYRAD [20] Monte Carlo using various pdfs in figure 10. With the exception of CTEQ2M the pdfs in the figure used the CDF run-1A W asymmetry data in the fits, which only extended to $|\eta| \sim 1$. It is apparent that the latest pdfs do not fit the new asymmetry data at high rapidity particularly well and a fit incorporating this new data is certainly desirable. For the run-1A CDF W mass analyses a limit was set on which pdfs were deemed acceptable by defining the

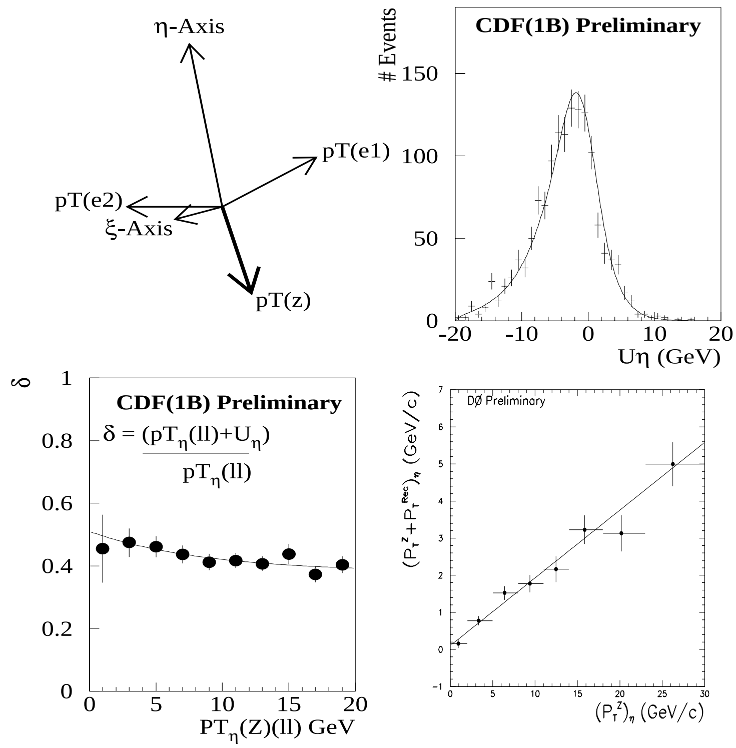

Figure 9: Top Left : Definition of the η axis. Top Right : $\vec{\mathrm{U}}$ projected along η axis for CDF $\mathrm{Z} \rightarrow \mu^+\mu^-$ events. Bottom Left : Response function as measured in CDF Z events (i.e. $U = (1-\delta)\mathrm{P}_{\mathrm{T}}^{\mathrm{W}}$). Bottom Right : Response function as measured in DØ, in this case δ is the gradient.

significance :

$$\xi = \frac{\overline{A}_{pdf} - \overline{A}_{data}}{\sigma(\overline{A}_{data})}$$

and considering only pdfs satisfying $|\xi| < 2$. All the latest pdfs (CTEQ-4 [21] and MRS-R [22]) satisfy this criteria. Consequently pending a more quantitative analysis of the pdf global fits and the inclusion of the run-1B CDF W asymmetry data in such fits a conservative estimate of the W mass uncertainty arising from pdfs is presently assigned.

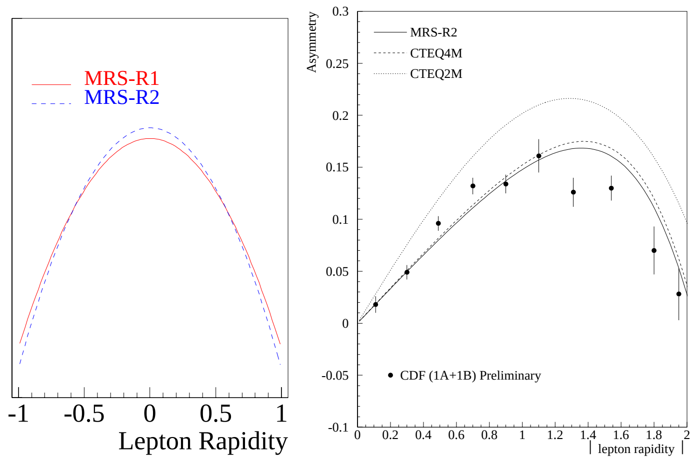

Figure 10: Left : The lepton rapidity distribution of simulated events (normalised to unit area) for two different pdfs. Right : The CDF measured asymmetry compared to three pdfs.

6.4 Mass determination

The W mass is obtained from a maximum likelihood fit of M_T templates generated at discrete values of M_W with Γ_W fixed at the SM value of 2.077 GeV. The templates also include the background distributions. The principal background in the muon channel arises from $Z \rightarrow \mu^+\mu^-$ events where the second muon is outside the tracking region and hence mimics at $\not{E}_T$ signal. The backgrounds in the CDF muon channel breakdown as : $Z \rightarrow \mu(\mu)$ (3.6%), $W \rightarrow \tau\nu \rightarrow \mu\nu\nu\nu$ (0.8%), QCD (0.4%) and cosmics (0.1%) – totaling 4.9% of the events in the M_T fit region, $65 < M_T < 100$. A failure to include the backgrounds in the simulation would shift the measured M_W by -170 MeV. In the DØ electron channel the principal background is from QCD background (1.5%) and also $Z \rightarrow e^+e^-$ events where the second electron is not detected (0.5%). The data and best fit distributions for both collaborations are shown in figure 11. The collaborations obtain mass values of :

$$\text{CDF} : M_W = 80.430 \pm 0.100\ (\text{stat.}) \pm 0.120\ (\text{syst.})\ \text{GeV}/c^2$$
$$\text{DØ} : M_W = 80.380 \pm 0.070\ (\text{stat.}) \pm 0.150\ (\text{syst.})\ \text{GeV}/c^2$$

The systematic errors are detailed in table 1. The results are preliminary and reductions in the systematic error are anticipated for the final results. Both collaborations perform

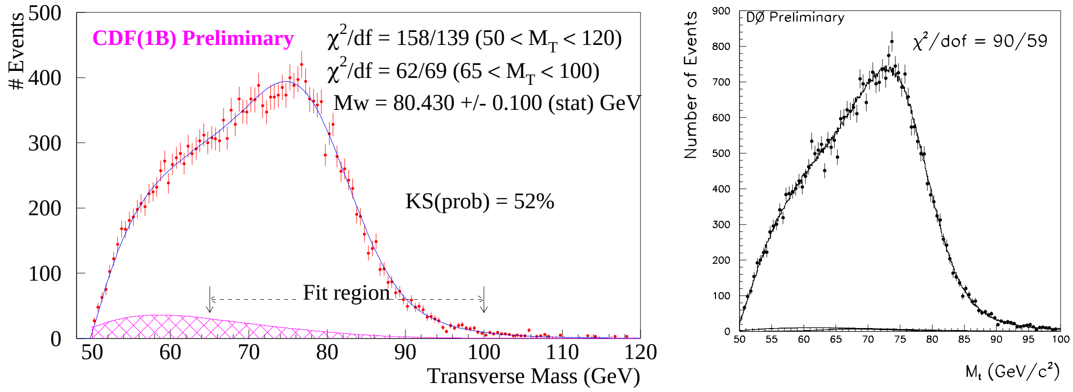

Figure 11: Left : The best fit in the $W \rightarrow \mu\nu$ channel for the CDF run-1B data. The fit is performed in the region $65 < M_T < 100$ GeV/c^2 and has 14723 events. Right : The best fit in the $W \rightarrow e\nu$ channel for the DØ run-1b data. The fit is performed in the region $60 < M_T < 90$ GeV/c^2 using a total of 32856 events. In both cases the shaded regions are the estimated backgrounds.

cross checks of the results by determining the W mass from the P_T^l and $\not{E}_T$ distributions. Although statistically less incisive than the M_T fits, the results serve as a valuable check on the validity of the assumed P_T^W distribution and recoil model. From such fits the collaborations obtain :

$$\begin{array}{lll} \mathrm{CDF}: & 80.510 \pm 0.135\ (\mathrm{stat.})\ (P_T^l)\ ; & 80.470 \pm 0.130\ (\mathrm{stat.})\ (\not{E}_T)\ \mathrm{GeV}/c^2 \\ \mathrm{D\O}\ : & 80.275 \pm 0.205\ (\mathrm{stat{+}syst.})\ (P_T^l)\ ; & 79.930 \pm 0.295\ (\mathrm{stat{+}syst.})\ (\not{E}_T)\ \mathrm{GeV}/c^2 \end{array}$$

showing good agreement with the values obtained from the M_T fits.

7 Combined Results

Both collaborations have combined their published results with these preliminary results and obtain :

CDF : $M_W = 80.375 \pm 0.120$ GeV/c^2 ; DØ : $M_W = 80.370 \pm 0.150$ GeV/c^2

The common errors have been accounted for in the averaging procedure, and in the case of CDF, the use of different pdfs in the analyses has been corrected for. Presently a

	Preliminary Uncertainty	ΔM_W^{μ} (MeV) **CDF 1B**	ΔM_W^{e} (MeV) **DØ 1B**
I.	Statistical	100	70
II.	Momentum/Energy Scale	40	80
III.	Other Systematics	115	130
	1. Resolution	25	30
	2. Input p_T^W	40	65 (+ pdf)
	3. Recoil modeling	90	60
	4. Parton distribution functions	25	–
	5. Selection bias	10	–
	6. Trigger bias/Efficiency	15	20
	7. QCD+QED corrections	20+20	20
	8. Backgrounds	25	15
	9. Fitting	10	5
	10. W-width	–	10
	11. Angle Scale	–	40
	12. Calorimeter Non Uniformity	–	10
	13. Luminosity dependence	–	70
TOTAL UNCERTAINTY		155	170

Table 1: The systematic errors for the preliminary run-1B W mass measurements from CDF and DØ.

conservative estimate of 50 MeV is used as the common uncertainty between CDF and DØ. It is expected that this will be reduced in the final analysis. With this common error the Tevatron W mass average[2] is : $M_W = 80.375 \pm 0.100$ GeV/c^2.

All W mass measurements to date are shown in figure 12. Assigning a common uncertainty of 50 MeV between the UA2 [24] result and the Tevatron value, and with the inclusion of the LEP2 [26, 27] and CCFR [25] measurements a world average value

[2]In March 1997 DØ updated their $W \rightarrow e\nu$ analysis [23] with $M_W = 80.450 \pm 0.120$ & M_W(DØ combined)$= 80.440 \pm 0.110$ GeV/c^2. The Tevatron average becomes : $M_W = 80.410 \pm 0.090$ GeV/c^2.

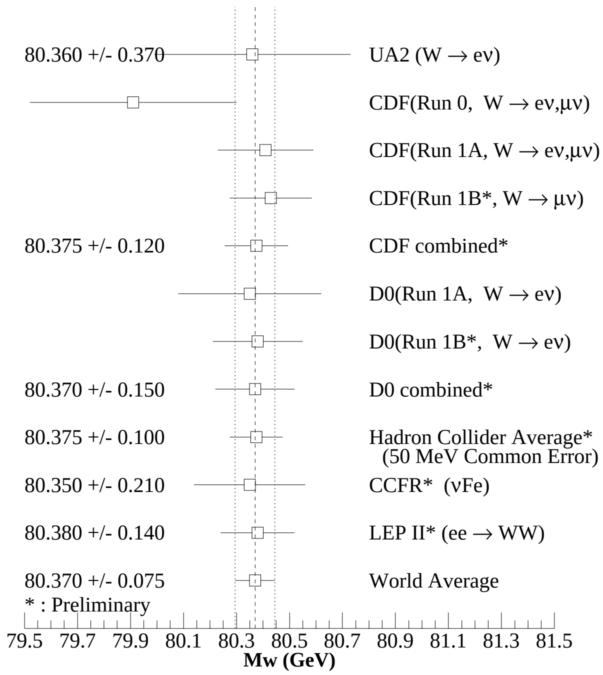

Figure 12: The W mass values from CDF, DØ, UA2, CCFR and the combined LEP2 measurement.

of [3] $M_W = 80.370 \pm 0.075$ GeV/c^2 is obtained. The present world average uncertainty on M_W is now considerably smaller than one year ago [28] and is becoming competitive with the top mass error in terms of a constraint on the Higgs mass. This is illustrated in figure 13 where the world average W mass and top mass are shown compared to the SM predictions for a variety of assumed Higgs masses varying from 100-1000 GeV/c^2. The constraint implied by the electroweak measurements at LEP and SLC is also shown. Good agreement with the SM model predictions is observed with a rather weak preference for a light Higgs mass. Before the LHC, new results from the Tevatron run-II on the top and W mass with errors of $\sim$ 3 GeV and $\sim$ 30 MeV respectively [29], along with a final LEP2 W mass uncertainty of $\mathcal{O}(50)$ MeV [30] should have been realised. The constraint on the predicted Higgs mass will then be rather tight and its confrontation with a direct measurement at the LHC will test the Standard Model or extensions thereof at a most fundamental level.

[3] With the updated DØ results the world average becomes $M_W = 80.390 \pm 0.070$ GeV/c^2.

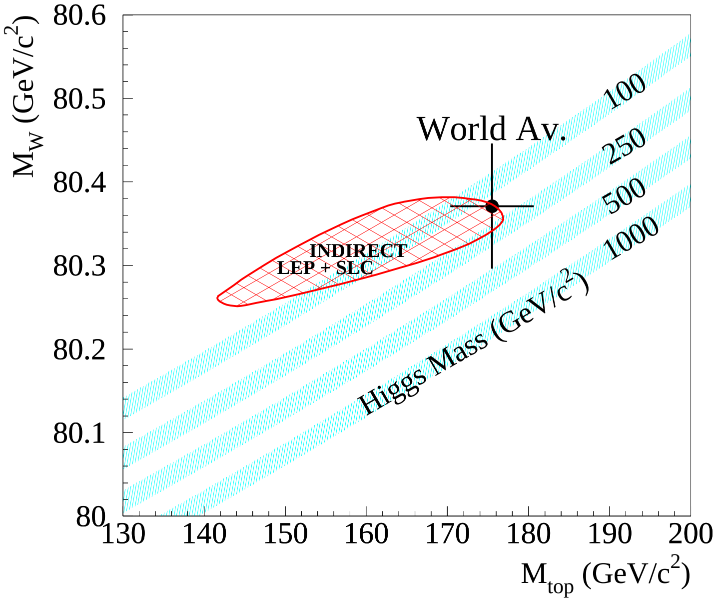

Figure 13: The world average W mass and top mass values compared to the SM predictions for Higgs masses in the range 100-1000 GeV. The constraint implied by the LEP and SLC electroweak measurements is also shown.

8 Conclusions

A large variety of electroweak measurements has been successfully undertaken at the Tevatron which provide many stringent tests of the SM, complementing those being made at other colliders. Extensions to the SM, manifest as substructure, neutral heavy gauge bosons and additional contributions to the W width have not been observed. The Tevatron experiments currently provide the most precise determination of the W mass which when combined with other results yields a W mass with an uncertainty of $\sim$ 75 MeV.

9 Acknowledgments

I would like to thank the organisers of the conference for the splendid arrangements, to Eric Flattum for providing many plots from the DØ experiment and to colleagues from both CDF and DØ for comments on this manuscript.

References

[1] CDF Collaboration, F. Abe *et al.*, Phys. Rev. Lett. 73 220 (1994);
CDF Collaboration, F. Abe *et al.*, Phys. Rev. D52 2624 (1995);
CDF Collaboration, F. Abe *et al.*, Phys. Rev. Lett. 76 3070 (1996).

[2] DØ Collaboration, S. Abachi *et al.*, Phys. Rev. Lett. 75 1456 (1995).

[3] R. Hamberg, W.L. van Neerven and T. Matsuura, Nucl. Phys. B359 343 (1991);
W.L. van Neerven and E.B. Zijlstra, Nucl. Phys. B382 11 (1992).

[4] J. L. Rosner, M. P. Worah and T. Takeuchi, Phys. Rev. D49 1363 (1994).

[5] Particle Data Group, R. M. Barnett *et al.*, Phys. Rev. D54 1 (1996).

[6] CDF Collaboration, F. Abe *et al.*, Phys. Rev. Lett. 74 341 (1995).

[7] CDF Collaboration, F. Abe *et al.*, Phys. Rev. Lett. 67 2418 (1991);
CDF Collaboration, F. Abe *et al.*, Phys. Rev. D49 1 (1994);
A. Bodek, on behalf of the CDF Collaboration, FERMILAB-CONF-96/381-E, Proceedings of the Cracow International Symposium on Radiative Corrections (CRAD96), Institute of Nuclear Physics, Krakow, Poland, August 1-5, 1996.

[8] E. Eichten, K. Lane, M. Peskin, Phys. Rev. Lett. 50 811 (1983).

[9] M. Pillai *et al.*, on behalf of the CDF Collaboration, Proceedings of the 1996 Divisional Meeting of the Division of Particles and Fields, American Physical Society, Minneapolis, MN, August 10-15, 1996.

[10] C. Gerber, on behalf of the DØ Collaboration, Proceedings of the 1996 Divisional Meeting of the Division of Particles and Fields, American Physical Society, Minneapolis, MN, August 10-15, 1996.

[11] CDF Collaboration, F. Abe *et al.*, Phys. Rev. Lett. 77 2616 (1996).

[12] J. L. Rosner, Phys. Rev. D54 1078 (1996).

[13] DØ Collaboration, S. Abachi *et al.*, hep-ex/9703008, Fermilab-Pub-97/059-E ; Top Mass = 173.3 ± 5.6 (stat) ± 6.2 (syst) GeV/c^2.
J. Lys, on behalf of the CDF Collaboration, FERMILAB-CONF-96/409-E, Proceedings of the 28th International Conference on High Energy Physics (ICHEP96),

Warsaw, Poland, July 25-31, 1996; Top Mass = 176.8 ± 4.4 (stat) ± 4.8 (syst) GeV/c^2.

[14] CDF Collaboration, F. Abe *et al.*, Phys. Rev. Lett. 75 11 (1995);
CDF Collaboration, F. Abe *et al.*, Phys. Rev. D52 4784 (1995);
DØ Collaboration, S. Abachi *et al.*, Phys. Rev. Lett. 77 3309 (1996).

[15] Eric Flattum, on behalf of the DØ Collaboration, FERMILAB-CONF-96/199-E, Proceedings of the XI Topical Workshop on $p\bar{p}$ Collider Physics, Padova, Italy, May 26-June 1, 1996.

[16] P.B. Arnold, R.P. Kauffman, Nucl. Phys. B349 381 (1991);
P.B. Arnold, M. Reno, Nucl. Phys. B319 37 (1989).

[17] G. Ladinsky and C.P. Yuan, Phys. Rev. D50 4239 (1994).

[18] C. Davies, W.J. Stirling, Nucl. Phys. B244 337 (1984) ;
C. Davies, B.R. Webber, W.J. Stirling, Nucl. Phys. B256 413 (1985).

[19] CDF Collaboration, F. Abe *et al.*., Phys. Rev. Lett. 74 850 (1995).
A. Bodek, on behalf of the CDF Collaboration, FERMILAB-CONF-96/219-E, Proceedings of DIS96 Conference, Rome, Italy, April 1996.

[20] W.T. Giele, E.W.N. Glover, David A. Kosower, Nucl. Phys. B403 633 (1993).

[21] CTEQ Collaboration, H.L. Lai *et al.*, Phys. Rev. D55 1280 (1997).

[22] A.D. Martin, R.G. Roberts, W.J. Stirling, Phys. Lett. B387 419 (1996).

[23] Presented by U. Heintz, Fermilab March 28 (1997), see :
http://www-d0.fnal.gov/public/wz/wmass/wmass.html.

[24] UA2 Collaboration, J. Alitti *et al.*, Phys. Lett. B276 354 (1992).

[25] CCFR Collaboration, K. McFarland *et al.*, FERMILAB-PUB-97-001/E.

[26] Results at $\sqrt{s}$ = 161 GeV :
ALEPH Collaboration, R. Barate *et al.*, CERN-PPE-97-025 ;
DELPHI Collaboration, P. Abreu *et al.*, Phys. Lett. B397 158 (1997);
L3 Collaboration, M. Acciarri *et al.*, Phys.Lett. B398 223 (1997);
OPAL Collaboration, K. Ackerstaff *et al.*, Phys. Lett. B389 416 (1996).

[27] Results at $\sqrt{s} = 172$ GeV :
W mass determinations at LEP II, Status for La Thuile/Moriond, see :
http://www.cern.ch/LEPEWWG/wmass/.

[28] World average $M_W = 80.34 \pm 0.150$ GeV/c^2, U. Heintz, on behalf of the DØ & CDF collaborations, FERMILAB-CONF-96/143-E, Proceedings of Les Recontres de Physique de la Vallée D'Aoste, La Thuile, Italy, March 3-9, 1996.

[29] U. Baur and M. Demarteau, FERMILAB-CONF-96/423, Proceedings of the 1996 DPF/DPB Summer Study on New Directions for High Energy Physics (Snowmass 96), Snowmass, Colorado, June 25 - July 12, 1996;
R. Frey *et al.*, FERMILAB-CONF-97/085, Proceedings of the 1996 DPF/DPB Summer Study on New Directions for High Energy Physics (Snowmass 96), Snowmass, Colorado, June 25 - July 12, 1996.

[30] Working Group Report : "Determination of the Mass of the W Boson", A. Ballestrero *et al.*, CERN/96-01. (1996).